The extremely low frequency electromagnetic stimulation selective for cancer cells elicits growth arrest through a metabolic shift

UNIVERSITÀ DEGLI STUDI DI TORINO

The extremely low frequency electromagnetic stimulation selective for cancer cells elicits growth arrest through a metabolic shift.

Loredana Bergandi [a], Umberto Lucia [b], Giulia Grisolia [b], Riccarda Granata [c], Iacopo Gesmundo [c], Antonio Ponzetto [c], Emilio Paolucci [d], Romano Borchiellini [b], Ezio Ghigo [c], Francesca Silvagno [a,*]

[a] Department of Oncology, University of Torino, Via Santena 5 bis, 10126 Torino, Italy

[b] Department of Energy, Politecnico di Torino, Corso Duca degli Abruzzi 24, 10129 Torino, Italy

[c] Department of Medical Sciences, University of Torino, Corso A.M. Dogliotti 14, 10126 Torino, Italy

[d] Department of Management and Production Engineering, Politecnico di Torino, Corso Duca degli Abruzzi 24, 10129 Torino, Italy

* Corresponding author.

Francesca Silvagno

Department of Oncology, University of Torino, Via Santena 5 bis, 10126 Torino.

E-mail address: francesca.silvagno@unito.it

Phone: +39-011-6705856

Fax: +39-011-6705845

Abstract

The efficacy of the very low frequency electromagnetic field in cancer treatment remains elusive due to a lack of explanatory mechanisms for its effect. We developed a novel thermodynamic model that calculates for every cell type the frequency capable of inhibiting proliferation. When this frequency was applied to two human cancer cell lines, it reduced their growth while not affecting healthy cells. The effect was abolished by the inhibition of calcium fluxes. We found evidences of an enhanced respiratory activity due to the increased expression of the elements of the respiratory chain and oxidative phosphorylation, both at the mRNA and protein level. The respiratory burst potentiated the production of reactive oxygen species but was not associated to increased levels of ATP, leading to the conclusion that the energy was readily spent in the adaptive response to the electromagnetic field. Taken together, our data demonstrate that, regardless of individual molecular defects, it is possible to control cancer cells with a specific irradiation that imposes a mitochondrial metabolic switch, regulating calcium fluxes and deleterious to cancer growth. This approach lays the foundations for a personalized cancer medicine.

Keywords: extremely low frequency electromagnetic field; cancer; thermodynamic approach; proliferation; mitochondrial respiration; calcium fluxes.

1. Introduction

Many recent studies have investigated the healing effects of the extremely low frequency electromagnetic field (ELF-EMF) both in vitro and in vivo, in the attempt to exploit the electromagnetism for medical purposes [1–3]. In particular the effects of ELF-EMF have been investigated in cancer [4–10]. These studies have used several different pattern of exposure, thus the heterogeneity of the given field in time, frequency and intensity has given fragmented results, mostly cell-specific. Among the many molecular events influenced by the electromagnetic radiation, the variation of ionic fluxes could be responsible for the activation of several signaling pathways modulated in exposed cancer cells [3,11,12].

Up to now a general explanation of the effects of ELF-EMF applied to oncology was missing. Recently, we have developed a biochemical thermodynamic model [13–17] able to predict the response of the biological system to the electromagnetic wave of very low frequency and intensity [18]. Our model is based on two pillars:

1. From a thermodynamic point of view, a living system is no more than an open system, kept in non-equilibrium thermodynamic states with its environment by the control of fluxes [19,20]. Energy and matter flow through the border of the system, while biochemical and biophysical transformations occur within the system, with a related net production of entropy. Any reaction generates a waste of heat towards the environment and we can describe cells as small systems which continuously dissipate energy to survive. We consider the cell living in a continuous non-equilibrium steady-state as an adaptive thermal engine, which converts energy into work by coupling metabolic and chemical reactions with transport processes and wasted heat into environment. Every cell process requires energy and mass fluxes, therefore the control of the energy conversion in the cell can represent a way to control the cell processes.

2. In physics and chemistry, resonance is the phenomenon in which a vibrating system or external force drives another system to oscillate with greater amplitude at specific frequencies. At resonant frequencies, small periodic driving forces have the ability to produce large amplitude oscillations,

due to the storage of vibrational energy. We have shown how a characteristic time of the biosystems exists and it holds to a frequency of electromagnetic or mechanical waves able to generate a resonant effect: this frequency can be evaluated by a resonant approach in heat transport [18,20]. By linking the two principles, we define the frequency of resonance at which we can change the energy and mass fluxes and consequently we can force cell behaviour.

From the First Law of thermodynamics, we can evaluate the heat wasted by the cell, considering the usual equation of heat exchange between a solid (soft matter) system and the fluid around it. It follows:

$$\rho c V \frac{dT}{dt} = \alpha A\left(T - T_0\right) \qquad (1)$$

where ρ is the density, c is the specific heat capacity, V is the cell volume, T is the temperature, t is time, α is the coefficient of convection between the blood and the cell membrane, A is the area of the surface cell, and 0 is the mean reference (the environment of the cells system). From equation (1) the frequency of resonance is obtained as [20]:

$$\nu = \frac{\alpha A}{\rho c V} \qquad (2)$$

which represents the natural frequency of a cell necessary to maintain the non-equilibrium steady-state. So, when we apply a perturbation to a cell with a mechanical or electromagnetic wave at its thermodynamic resonant frequency, obtained by using the Constructal Law analysis [20], we expect to force the cell state and to produce an amplification of the heat exchanged. The thermodynamic resonant frequency is expressed in terms of physical properties of the systems but also by the geometrical characteristics V/A, the shape of the bio-system [20]. This quantity results the fundamental property in the numerical evaluation because the numerical results are particular sensitive to any approximation of this quantity. This approach has been theoretically evaluated and experimentally verified in vitro [18]. The biochemical interpretation of the thermodynamic model

explains the reduced cell growth observed in many cell lines exposed to specific ELF-EMF frequencies [18].

In the present work we further investigated the effects of the radiation on cell growth and metabolism, and the mechanisms mediating the cellular response to the ELF electromagnetic wave. We irradiated with specifically calculated frequencies two models of human cancer: the triple negative human breast cancer (MDA-MB-231 cell line) and the human malignant pleural mesothelioma (MSTO-211H cell line); these cells are different in morphology and proliferation rate and are both representative of cancers with poor prognosis. Moreover we tested a specific frequency of the ELF-EMF on a model of human healthy tissue, the primary human umbilical vein endothelial cells (HUVEC). In all models, we were able to select the frequency and intensity of the electromagnetic wave affecting specifically only one type of cell. We investigated the effects of the applied field on proliferation and energy metabolism; moreover, we assessed the possible involvement of ionic fluxes in the interactions between the cancer cell and the electromagnetic field.

2. Materials and methods

2.1. Cell cultures and treatments

Two models of aggressive human cancer were used in this study: MDA-MB-231 is a human triple-negative breast adenocarcinoma cell line and MSTO-211H is a human biphasic malignant pleural mesothelioma cell line. As a non malignant counterpart, the human mammary non-tumorigenic epithelial cell line MCF-10A and the human bronchial epithelial cells Beas-2B were analysed. All cell lines were obtained from the American Type Culture Collection (ATCC; Rockville, MD, USA). Primary human umbilical vein endothelial cells (HUVEC) were kindly provided by Dr. Castelli, University of Torino, Italy. The cells were grown as a subconfluent monolayer in RPMI (MSTO-211H, MCF-10A and BEAS-2B) as previously described [21] or in DMEM with 4.5 g/l glucose medium (MDA-MB-231) or 199 medium with heparin (10000 U/ml) and human FGF-basic (1000

ng/ml) (HUVEC cells) containing 2 mM L-glutamine, 1% (v/v) antibiotics (penicillin/streptomycin solution) and 10 % (v/v) fetal bovine serum (FBS) at 37°C in a humidified atmosphere containing 5% CO_2. For calcium experiments, cells were cultured in medium without calcium or in standard medium with calcium (growth medium, GM) in the absence or presence of 10 µM 1,2-bis (2 aminophenoxy)ethane-N,N,N",N (BAPTA-AM), 10 µM nifedipine and 10 µM verapamil. Unless otherwise specified, reagents were purchased from Sigma Aldrich (Milan, Italy).

The cells were seeded in 96-multiwell plates for proliferation assays or 6-multiwell plates for cell cycle, JC-1 and PCR analysis, or 100 mm dishes for protein extraction; the cells were continuously exposed to ELF-EMF throughout the experiments, whereas control cells were grown in the same incubator under standard conditions.

2.2 ELF-EMF exposure system

The experimental setup has been described previously [18,22] and it is shown in supplementary Figure S1. Briefly, the cell culture dishes were placed in the central part of the apparatus, made of two independent couples of coaxial coils made of 200 loops. The experimental setup was placed in the incubator inside a box that shielded the apparatus from the background magnetic field. The outer coils were supplied with a direct current (DC) that provided a constant magnetic field of 45 µT, which is the average value of the earth's magnetic field. The inner coils were connected to an AC current generator that produced a sine wave signal at the specific frequencies calculated by the mathematical model and at the intensity of 100 µT .

2.3. Proliferation assay

The effect of ELF-EMF on the cell growth of the different human cancer cell lines was determined in a 96-multiwell plate by crystal violet staining, as previously reported [18] or by BrdU incorporation assay, after two, three and four days of incubation with or without exposure to ELF-EMF.. HUVEC were poorly stained by the crystal violet method, and the detection by

spectrophotometer was inadequate to quantify these cells; therefore, the more sensitive BrdU assay was chosen. The crystal violet assay evaluated proliferation as number of cells in the well (proportional to the staining) whereas the incorporation of BrdU estimated the number of duplicating cells at the time of the assay; the proliferation rate was determined by the colorimetric Cell Proliferation ELISA BrdU kit (Roche Applied Science, Penzberg, German) following the manufacturer's instructions. In experiments evaluating the role of calcium fluxes, the BrdU assay was carried out on cells cultured for two days in standard conditions or with pharmacological treatments in absence or presence of ELF-EMF exposure. The data collected from 12 wells (crystal violet) or 6 wells (BrdU) were averaged for each experimental condition, and each experiment was repeated three times.

2.4. Real-time polymerase chain reaction (qRT-PCR)

MDA-MB231 and MSTO-211H cells were seeded on 6-multiwell plates and they were cultured for 2 days in standard conditions or exposed to ELF-EMF. The cells were washed with PBS and total RNA was extracted with TRIzol® (Invitrogen, Thermo Fisher Scientific, Waltham, MA, USA). One μg of total RNA were reversely transcribed into cDNA, in a final volume of 20 μl, using the High-Capacity cDNA Reverse Transcription Kit (Thermo Fisher Scientific, Waltham, MA, USA) according to the manufacturer's instructions. The RT-PCR primers were designed with NCBI/ Primer-BLAST, synthesized by Sigma (Milan, Italy). Quantitative PCR was carried out in a final volume of 20 μl using the SensiFAST™ SYBR® Hi-ROX Kit (Bioline Srl, Trento, Italy) with specific primers for the quantitation of the following human genes: cytochrome c oxidase subunit 2 (COXII, fwd 5'-TCTGGTCAGCCCAACTCTCT-3', rev 5'-CCTGTGATCCACCAGAAGGT-3'), cytochrome c oxidase subunit 4 (COXIV, fwd 5'-CGAGCAATTTCCACCTCTGT-3', rev 59-GGTCAGCCGATCCATATAA-39), ATP synthase subunit beta (ATP5B, fwd 5'-GTGGGCTATCAGCCTACCCT-3', rev 5'-CAAGTCATCAGCAGGCACAT -3'), mitochondrial ATP synthase F0 subunit 6 (MT-ATP6, fwd 5'-CCAATAGCCCTGGCCGTAC-3', rev 5'-

CGCTTCCAATTAGGTGCATGA-3'), and beta 2-microglobulin (β2M, fwd 5'-AGCAAGGACTGGTCTTTCTATCTC-3', rev 5'-ATGTCTCGATCCCACTTAACTA-3'). PCR amplification was 1 cycle of denaturation at 95°C for 2 min, 40 cycles of amplification including denaturation at 95°C for 5 sec and annealing/extension at 60°C for 30 sec. The quantification of each sample was carried out comparing each PCR gene product with β2M, used as reference gene to normalize the cDNA in different samples. Data were analysed using the 2_ΔΔCT method. Analyzed transcripts exhibited high linearity amplification plots ($r > .98$) and similar PCR efficiency, confirming that the expression of each gene could be directly compared. The specificity of PCRs was confirmed by melt curve analysis. Nonspecific amplifications were never detected.

2.5. Measurement of the mitochondrial membrane potential (ΔΨm) JC-1

JC-1 (5,5′,6,6′-tetrachloro-1,1′,3,3′-tetraethylbenzimidazolylcarbocyanine iodide), a mitochondrial dye staining mitochondria in living cells in a membrane potential-dependent fashion, was used to determine ΔΨm by flow cytometry, as previously reported [23]. The potential-dependent accumulation in mitochondria is indicated by a fluorescence emission shift from green to red, due to the formation of red fluorescent J-aggregates. Consequently, the enhanced mitochondrial activity is indicated by an increase in the red/ green fluorescence intensity ratio (FL2/FL1 channels of flow cytometer).

2.6. Measurement of mitochondrial ATP level

MDA-MB231 and MSTO-211H cells were seeded on 6-multiwell plates and then cultured for two days in standard conditions or exposed to ELF-EMF. Mitochondria were prepared and analysed as previously reported [22]. The amount of mitochondrial ATP was measured with the ATP Bioluminescent Assay Kit (FL-AA, Sigma Aldrich, Milan, Italy). ATP was quantified as relative light units (RLU) and data were converted into nmol ATP/mg mitochondrial proteins. Experiments were performed in triplicates and repeated three times.

2.7. Western blot analysis

MDA-MB231 and MSTO-211H cells were seeded on 6-multiwell plates and cultured for two days in standard conditions or exposed to ELF-EMF. Subcellular fractionation and western blotting analyses of mitochondrial proteins were carried out as previously described [24]. Fifty μg of mitochondrial extracts were subjected to 12 % SDS-PAGE, transferred to PVDF membrane and probed with the OXPHOS Human WB Antibody Cocktail (Abcam, Cambridge, UK) containing 5 mouse monoclonal antibodies (diluted 1:500 in PBS-BSA 1%) against Complex I subunit NDUFB8, Complex II subunit 30kDa, Complex III subunit Core 2, Complex IV subunit II, and ATP synthase subunit alpha. Mouse anti-VDAC antibody (diluted 1:500 in 1% PBS-BSA) (anti-porin 31HL) was purchased from Calbiochem and was used to check the equal protein loading. Mouse anti-actin antibody (Santa Cruz, sc-8432) was diluted 1:1000 in 1% PBS-BSA and was used to confirm the quality of mitochondrial purification. Densitometric analysis was carried out using Image J software (http://rsbweb.nih.gov/ij/).

2.8. Measurement of total cellular ROS production

MDA-MB231 and MSTO-211H cells were seeded on 6-multiwell plates and cultured for two days in standard conditions or exposed to ELF-EMF. Unstimulated cell were also treated for three hours with 100 μM menadione, which is a known generator of ROS, as positive control of the assay. The cells were washed, detached in 1 ml PBS by scraping, resuspended in 1 ml of PBS and loaded for 15 min with 10 μM 2′,7′-dichlorodihydrofluorescein diacetate (DCFH-DA). DCFH-DA is a cell-permeable probe that is cleaved by nonspecific intracellular esterases to form DCFH, which is further oxidized by ROS to form the fluorescent compound dichlorofluorescein (DCF). After the incubation, cells were washed twice with PBS to remove excess probe, and total DCF fluorescence were determined at an excitation wavelength of 504 nm and an emission wavelength of 529 nm, using a Packard EL340 microplate reader (Bio-Tek Instruments, Winooski, VT). The fluorescence

value was normalized to the protein content and expressed as relative to control. Experiments were performed in triplicates and repeated three times.

2.9 Cell cycle analysis and lactate dehydrogenase (LDH) activity

The protocols used in this study are described in Supplementary Methods.

2.10. Statistical analysis

Statistical analysis of data was performed using ANOVA test with Tukey's post-hoc correction or by an unpaired two-tailed Student's t-test, as required. P values <0.05 were considered significant and indicated. All data were expressed as mean ± S.D of three independent experiments.

3. Results

3.1 ELF-EMF exposure inhibited cell growth and decreased cells in the S-phase

The frequency of the ELF-EMF used for each cellular type was calculated by our mathematical model as previously published, after evaluation of cell morphology and size [18]. The efficacy of the selected exposure was first of all verified as arrest of cell growth.

Cell proliferation was assessed in breast cancer cells MDA-MB-231 and in biphasic pleural mesothelioma MSTO-211H cell lines, in their non malignant counterpart (the mammary non-tumorigenic epithelial cell line MCF-10A and the bronchial epithelial cells Beas-2B) and in healthy endothelial HUVEC cells. After four days of exposure to ELF-EMF, crystal violet staining of control and treated cells evaluated the number of cells, whereas HUVEC cells were investigated by BrdU assay. The treatment significantly inhibited cell growth only at a frequency specific for each cell type, namely 6 Hz for MDA-MB-231 cells, 16 Hz for MSTO-211H and 13 Hz for HUVEC (Fig. 1). The stimulation did not affect the non-malignant counterpart.

We further analysed the characteristics of growth inhibition in cancer cells. We carried out time-course experiments evaluating the cell growth up to four days of exposure to ELF-EMF. The BrdU assay, which labels replicating cells and thus measures the proliferation rate, confirmed that the selected frequencies decreased the number of actively proliferating MDA-MB-231 and MSTO-211H cells exposed to the ELF-EMF compared to control; the effect was already evident after two days of exposure and was maintained up to four days (Fig. 2A) . By crystal violet staining we could detect the reduction in proliferation at day three and four, whereas the difference at day two was too small to be detectable by this method of cell number quantification (Fig. 2B). We observed a reduced growth even after eight days of exposure to ELF-EMF, as assessed by crystal violet staining (Fig. 2C), which detected a number of cells lower than what quantified after four days of exposure ($p<0,0001$). Moreover, when the distribution of MDA-MB-231 and MSTO-211H cells in the various stages of the cell cycle was examined, we found that ELF-EMF treatment for 2 days significantly and selectively decreased the cells in S phase, whereas the other phases showed variable not significant changes (Fig. 2D, 2E). Not only this observation reinforces the results of proliferation analysis, but it also substantiates its significance; in fact the decrease of S phase upon ELF-EMF exposure is even more evident than the decrease of proliferation rate measured by BrdU assay at the same time point, because it is based on the observation of cells accumulated in each phase over time.

3.2 The exposure to ELF-EMF inhibited the proliferation of human cancer cell lines by the modulation of calcium efflux

Among the ionic fluxes that could be modulated by ELF-EMF in our experimental model, we decided to investigate the involvement of calcium fluxes. In fact it has been reported that the ELF-EMF may affect the calcium ions efflux from various cells [5,12–14]. The two cell lines were treated in order to abolish the calcium fluxes: they were incubated with a medium without calcium, or with 10 μM BAPTA-AM (a cell-permeant chelator which is highly selective for Ca2+ over

Mg2+), or with 10 µM nifedipine or 10 µM verapamil (two calcium channel blockers). The exposure to the ELF-EMF reduced the proliferation of both cell lines when they were incubated in normal growth medium (GM), but the effect was lost in the presence of the drugs: in fact, in every pharmacological treatment we could not detect a difference in proliferation between cells grown in standard condition or exposed to ELF-EMF (Fig. 3). From these results we concluded that the inhibitory effect of the field was mediated by calcium fluxes, because when we perturbed the homeostasis of this ion the effect was lost.

3.3 Mitochondrial respiration is increased by ELF-EMF exposure

Our published biochemical theoretical model hypothesizes that the ELF-EMF affects ion fluxes and elicits a homeostatic response to compensate and minimize the perturbation. The energy necessary to restore ionic gradients is produced mainly in the mitochondria as ATP. Based on these considerations, we investigated the possible alterations in mitochondrial respiratory activity and in the modulation of the complexes of respiratory chain and oxidative phosphorylation (OXPHOS). First of all, mRNA transcription and protein expression of mitochondrial respiratory complexes was evaluated in MDA-MB-231 and MSTO-211H. After 2 days of ELF-EMF exposure, we found an increased mRNA level of two subunits of complex IV: cytochrome c oxidase subunit 2 (COX2) and subunit 4 (COX4), whose transcripts are of mitochondrial (the former) and nuclear (the latter) origin. Moreover also two subunits of ATP synthase were upregulated in their nuclear (ATP5B) and mitochondrial transcription (MT-ATP6) (Fig. 4A). Accordingly, after ELF-EMF exposure we also detected an increase in protein expression of complex I, II, III, IV and ATP synthase in treated cells compared to control (Fig. 4B). A representative blot is shown in supplementary Figure S2.
The increased expression of the respiratory complexes was associated with a significant enhancement of mitochondrial membrane potential ($\Delta\Psi m$), a major parameter which reflects mitochondrial functionality and it is dependent on electron transport chain activity. As shown in Fig. 5A, after 2 days of ELF-EMF exposure we observed an increased mitochondrial respiratory

activity in treated cells, as measured by cytofluorimetric evaluation of mitochondrial membrane potential with JC-1. Nevertheless, when we evaluated the impact of ELF-EMF on ATP synthesis we found no differences in ATP levels (Fig. 5B); altogether the data on expression and activity suggested that the cells exposed to ELF-EMF potentiated the respiratory chain and the coupled ATP synthase but readily spent ATP to restore the optimal cellular gradients. Furthermore, the cytosolic LDH activity, used as an indirect evaluation of the glycolytic rate [25,26], did not change after ELF-EMF exposure (Fig. 5C), therefore we excluded the contribution of the cytosolic energy pathway in the metabolic response to ELF-EMF.

Because one of the consequences of the respiratory burst is the production of ROS, we were interested in checking whether ELF-EMF exposure induced any effect on ROS production in our cellular models. When MDA-MB-231 and MSTO-211H cells were treated for two days with ELF-EMF we observed the rise in the intracellular levels of ROS, measured as the increase of dichlorofluorescein-derived fluorescence, compared with non-stimulated cells (Fig. 5D). The enhanced respiratory activity associated with the significant increase in ROS production in treated cells support the stimulation of the mitochondrial compartment triggered by the electromagnetic field.

4. Discussion

In this study we show the decrease of proliferation of two cancer cell lines exposed to ELF frequencies specific for the single cell line, as calculated by our novel thermodynamic approach. Our theoretical model is able to select the frequencies that inhibit the growth of several cancer cell lines with a specificity related to the characteristics of each cell population [18]. When the target cell is exposed to an electromagnetic wave at its thermodynamic resonant frequency, its non-equilibrium steady-state is perturbed. The novelty of our approach relies exactly on the principle of shifting the cellular equilibrium; we assume that the biological system adapts to the variations

imposed by the ELF-EMF by spending energy to restore the optimal gradients perturbed by ionic fluxes, reaching a new equilibrium that interferes with cell growth. In this study we demonstrated that the molecular basis of our biochemical thermodynamic model can be explained by the impact of ELF-EMF on the mitochondrial energy machinery. We validated the robustness of our mathematical model by calculating the frequencies able to affect two human cell lines representative of two aggressive and incurable tumors: the triple negative breast cancer and the malignant pleural mesothelioma. The frequencies used were specific for each cancer cell type, whereas the non malignant counterpart was not targeted. Interestingly, we demonstrated that a human healthy endothelial cell culture was unaffected by tumor-specific electromagnetic waves and was sensitive to a different frequency, giving evidences that this approach would be not only safe for healthy tissues but it could also specifically hamper tumor angiogenesis. The cancer cells responded to the specific electromagnetic radiation by reducing proliferation rate and shifting the cell cycle already after two days of exposure; the stimulation can be defined as specific, quickly effective and sustained even in the long term, since we tested the inhibition of growth up to eight days. Next we set out to investigate which ionic fluxes could be involved in the stimulation triggered by the specific electromagnetic field. We focused our analysis on calcium fluxes, because several previous studies have demonstrated the influence of ELF-EMF on calcium homeostasis [27–32], moreover the control of intracellular levels of calcium is of paramount importance for all the tissues, and the cells spend a lot of energy to keep the ATP-dependent calcium channels operative. Indeed, our experiments aimed at reducing the intracellular variation of free calcium demonstrated that the inhibition of calcium fluxes abolished the effect of ELF-EMF on cancer cells. The energy required to adapt to the electromagnetic stimulation is produced in the mitochondria, because we found the evidences of an enhanced respiratory activity due to the increased expression of the elements of the respiratory chain and OXPHOS (both at the mRNA and protein level). It is interesting to note that ELF-EMF induced the synthesis of both the nuclear and the mitochondrial transcripts in order to potentiate the expression and activity of the whole respiratory machinery. We

reckon that the effect of the electromagnetic wave is not directed on a specific gene regulation but rather it is the result of an enhanced energy request. The coupled induction of both the respiratory complex and the ATP synthase subunits not associated to increased levels of ATP lead us to conclude that the energy is readily spent, reinforcing our hypothesis that the ELF-EMF forces the cells to adapt to the variation of fluxes. The link between electromagnetic stimulation, calcium flux and respiratory induction is supported by many studies that demonstrated a direct role of calcium in driving mitochondrial metabolism and ATP production [33–35]. A further evidence of the increased respiratory activity was found in the analysis of intracellular levels of ROS. Their increment after stimulation with ELF-EMF can be ascribed to the amplified leakage of electrons that represents a side-effect of the respiratory burst. Some other studies have shown the stimulating effects of ELF-EMF on ROS production in cancer cells [36,37], but we demonstrated for the first time the association of ROS production with the stimulation of the mitochondrial metabolism triggered by the electromagnetic field.

Many recent works support the idea that increasing respiratory chain activity inhibits growth in cancer cells [23,38,39], and in a previous study we described the link between enhanced respiratory activity and reduced cell growth upon ELF-EMF exposure [22]. The negative effects of the ELF electromagnetic fields on cancer proliferation demonstrated in this study can be interpreted as a consequence of the intensified activity of the respiratory chain, leading to the stimulation of oxidative catabolism to the detriment of the biosynthetic pathways; thus the cancer cells are not supported in their demand of mitochondrial biosynthetic intermediates essential to proliferation. The exposure to specific frequencies of ELF-EMF changes the conversion of energy of the target cells, as schematized in Fig. 6. In order to survive, the cells are forced to dissipate energy and are not able to proliferate.

This study provides formal proof of the possibility of using ELF-EMF as a metabolic approach in the fight against cancer. Likewise many cutting edge strategies targeting cancer metabolism, the

aim is to find a safe treatment that shifts the metabolic activity of cancer cells and hampers their ability to proliferate. Future studies in vivo are warranted to reach this goal.

In conclusion, in this study we validated the efficacy and specificity of the treatment of cancer cells with ELF-EMF on two models of aggressive and incurable cancer. We described the molecular basis of the growth inhibition that do not rely on the control of signaling pathways of a specific cancer type; rather, cancer cells are affected in their proliferation as the result of a mitochondrial metabolic switch necessary to control calcium fluxes and deleterious to cancer growth.

The evidences brought forward in this study support the general validity of our theoretical model that calculates the optimal frequency and intensity of the radiation on the basis of cell morphology, regardless of the molecular defects of cancer cells, and thus lays the foundations for future studies in vivo that could lead to personalized cancer treatments.

Conflicts of interest

The authors have no conflicts of interest to declare.

Declarations of interest

None.

Acknowledgements

This research was funded by a grant from Politecnico di Torino. LB was supported by Politecnico di Torino. We thank Dr. Ada Castelli (University of Torino) for preparing and providing HUVEC cells.

References

[1] M.H. Repacholi, B. Greenebaum, Interaction of static and extremely low frequency electric and magnetic fields with living systems: health effects and research needs, Bioelectromagnetics. 20 (1999) 133–160.

[2] M.T. Santini, G. Rainaldi, P.L. Indovina, Cellular effects of extremely low frequency (ELF) electromagnetic fields, Int. J. Radiat. Biol. 85 (2009) 294–313. doi:10.1080/09553000902781097.

[3] I. Verginadis, A. Velalopoulou, I. Karagounis, Y. Simos, D. Peschos, S. Karkabounas, A. Evangelou, Beneficial effects of electromagnetic radiation in cancer, in: Electromagn. Radiat., InTech, 2012.

[4] A. Koziorowska, M. Romerowicz-Misielak, P. Sołek, M. Koziorowski, Extremely low frequency variable electromagnetic fields affect cancer and noncancerous cells in vitro differently: Preliminary study, Electromagn. Biol. Med. 37 (2018) 35–42. doi:10.1080/15368378.2017.1408021.

[5] C.A. Buckner, A.L. Buckner, S.A. Koren, M.A. Persinger, R.M. Lafrenie, Inhibition of Cancer Cell Growth by Exposure to a Specific Time-Varying Electromagnetic Field Involves T-Type Calcium Channels, PLOS ONE. 10 (2015) e0124136. doi:10.1371/journal.pone.0124136.

[6] S. Delle Monache, A. Angelucci, P. Sanità, R. Iorio, F. Bennato, F. Mancini, G. Gualtieri, R.C. Colonna, Inhibition of angiogenesis mediated by extremely low-frequency magnetic fields (ELF-MFs), PloS One. 8 (2013) e79309. doi:10.1371/journal.pone.0079309.

[7] B. Glück, V. Güntzschel, H. Berg, Inhibition of proliferation of human lymphoma cells U937 by a 50 Hz electromagnetic field, Cell. Mol. Biol. Noisy--Gd. Fr. 47 Online Pub (2001) OL115-117.

[8] Z. Akbarnejad, H. Eskandary, C. Vergallo, S.N. Nematollahi-Mahani, L. Dini, F. Darvishzadeh-Mahani, M. Ahmadi, Effects of extremely low-frequency pulsed electromagnetic fields (ELF-PEMFs) on glioblastoma cells (U87), Electromagn. Biol. Med. 36 (2017) 238–247. doi:10.1080/15368378.2016.1251452.

[9] L.-Q. Yuan, C. Wang, K. Zhu, H.-M. Li, W.-Z. Gu, D.-M. Zhou, J.-Q. Lai, D. Zhou, Y. Lv, S. Tofani, X. Chen, The antitumor effect of static and extremely low frequency magnetic fields against nephroblastoma and neuroblastoma, Bioelectromagnetics. 39 (2018) 375–385. doi:10.1002/bem.22124.

[10] H. Jimenez, C. Blackman, G. Lesser, W. Debinski, M. Chan, S. Sharma, K. Watabe, H.-W. Lo, A. Thomas, D. Godwin, W. Blackstock, A. Mudry, J. Posey, R. O'Connor, I. Brezovich, K. Bonin, D. Kim-Shapiro, A. Barbault, B. Pasche, Use of non-ionizing electromagnetic fields for the treatment of cancer, Front. Biosci. Landmark Ed. 23 (2018) 284–297.

[11] R.H.W. Funk, T. Monsees, N. Ozkucur, Electromagnetic effects - From cell biology to medicine, Prog. Histochem. Cytochem. 43 (2009) 177–264. doi:10.1016/j.proghi.2008.07.001.

[12] D.J. Panagopoulos, A. Karabarbounis, L.H. Margaritis, Mechanism for action of electromagnetic fields on cells, Biochem. Biophys. Res. Commun. 298 (2002) 95–102.

[13] U. Lucia, Bioengineering thermodynamics of biological cells, Theor. Biol. Med. Model. 12 (2015) 29. doi:10.1186/s12976-015-0024-z.

[14] U. Lucia, G. Grisolia, Second law efficiency for living cells, Front. Biosci. Sch. Ed. 9 (2017) 270–275.

[15] U. Lucia, G. Grisolia, A. Ponzetto, T.S. Deisboeck, Thermodynamic considerations on the role of heat and mass transfer in biochemical causes of carcinogenesis, Phys. Stat. Mech. Its Appl. 490 (2018) 1164–1170. doi:10.1016/j.physa.2017.08.075.

[16] U. Lucia, Thermodynamics and cancer stationary states, Phys. Stat. Mech. Its Appl. 392 (2013) 3648–3653. doi:10.1016/j.physa.2013.04.033.

[17] U. Lucia, A. Ponzetto, T.S. Deisboeck, Constructal approach to cell membranes transport: Amending the 'Norton-Simon' hypothesis for cancer treatment, Sci. Rep. 6 (2016) 19451. doi:10.1038/srep19451.
[18] U. Lucia, G. Grisolia, A. Ponzetto, F. Silvagno, An engineering thermodynamic approach to select the electromagnetic wave effective on cell growth, J. Theor. Biol. 429 (2017) 181–189. doi:10.1016/j.jtbi.2017.06.029.
[19] C. Bustamante, Y.R. Chemla, N.R. Forde, D. Izhaky, Mechanical processes in biochemistry, Annu. Rev. Biochem. 73 (2004) 705–748. doi:10.1146/annurev.biochem.72.121801.161542.
[20] U. Lucia, G. Grisolia, Constructal law and ion transfer in normal and cancer cells, Proceedings of the Romanian Academy, series A, Special Issue (2018) 213-218.
[21] T. Villanova, I. Gesmundo, V. Audrito, N. Vitale, F. Silvagno, C. Musuraca, L. Righi, R. Libener, C. Riganti, P. Bironzo, S. Deaglio, M. Papotti, R. Cai, W. Sha, E. Ghigo, A.V. Schally, R. Granata, Antagonists of growth hormone-releasing hormone (GHRH) inhibit the growth of human malignant pleural mesothelioma, Proc. Natl. Acad. Sci. U. S. A. (2019). doi:10.1073/pnas.1818865116.
[22] M. Destefanis, M. Viano, C. Leo, G. Gervino, A. Ponzetto, F. Silvagno, Extremely low frequency electromagnetic fields affect proliferation and mitochondrial activity of human cancer cell lines, Int. J. Radiat. Biol. 91 (2015) 964–972. doi:10.3109/09553002.2015.1101648.
[23] M. Consiglio, M. Destefanis, D. Morena, V. Foglizzo, M. Forneris, G. Pescarmona, F. Silvagno, The vitamin D receptor inhibits the respiratory chain, contributing to the metabolic switch that is essential for cancer cell proliferation, PloS One. 9 (2014) e115816. doi:10.1371/journal.pone.0115816.
[24] F. Silvagno, M. Consiglio, V. Foglizzo, M. Destefanis, G. Pescarmona, Mitochondrial translocation of vitamin D receptor is mediated by the permeability transition pore in human keratinocyte cell line, PloS One. 8 (2013) e54716. doi:10.1371/journal.pone.0054716.
[25] E.A. Mandujano-Tinoco, J.C. Gallardo-Pérez, A. Marín-Hernández, R. Moreno-Sánchez, S. Rodríguez-Enríquez, Anti-mitochondrial therapy in human breast cancer multi-cellular spheroids, Biochim. Biophys. Acta. 1833 (2013) 541–551. doi:10.1016/j.bbamcr.2012.11.013.
[26] G. Lin, G. Andrejeva, A.-C. Wong Te Fong, D.K. Hill, M.R. Orton, H.G. Parkes, D.-M. Koh, S.P. Robinson, M.O. Leach, T.R. Eykyn, Y.-L. Chung, Reduced Warburg effect in cancer cells undergoing autophagy: steady- state 1H-MRS and real-time hyperpolarized 13C-MRS studies, PloS One. 9 (2014) e92645. doi:10.1371/journal.pone.0092645.
[27] R. Karabakhtsian, N. Broude, N. Shalts, S. Kochlatyi, R. Goodman, A.S. Henderson, Calcium is necessary in the cell response to EM fields, FEBS Lett. 349 (1994) 1–6.
[28] J. Zhou, G. Yao, J. Zhang, Z. Chang, CREB DNA binding activation by a 50-Hz magnetic field in HL60 cells is dependent on extra- and intracellular Ca(2+) but not PKA, PKC, ERK, or p38 MAPK, Biochem. Biophys. Res. Commun. 296 (2002) 1013–1018.
[29] P.K. Manikonda, P. Rajendra, D. Devendranath, B. Gunasekaran, null Channakeshava, R.S.S. Aradhya, R.B. Sashidhar, C. Subramanyam, Influence of extremely low frequency magnetic fields on Ca2+ signaling and NMDA receptor functions in rat hippocampus, Neurosci. Lett. 413 (2007) 145–149. doi:10.1016/j.neulet.2006.11.048.
[30] J.J. Carson, F.S. Prato, D.J. Drost, L.D. Diesbourg, S.J. Dixon, Time-varying magnetic fields increase cytosolic free Ca2+ in HL-60 cells, Am. J. Physiol. 259 (1990) C687-692. doi:10.1152/ajpcell.1990.259.4.C687.
[31] G.P. Pessina, C. Aldinucci, M. Palmi, G. Sgaragli, A. Benocci, A. Meini, F. Pessina, Pulsed electromagnetic fields affect the intracellular calcium concentrations in human astrocytoma cells, Bioelectromagnetics. 22 (2001) 503–510.
[32] E. Lindström, P. Lindström, A. Berglund, E. Lundgren, K.H. Mild, Intracellular calcium oscillations in a T-cell line after exposure to extremely-low-frequency magnetic fields with variable frequencies and flux densities, Bioelectromagnetics. 16 (1995) 41–47.

[33] E.J. Griffiths, G.A. Rutter, Mitochondrial calcium as a key regulator of mitochondrial ATP production in mammalian cells, Biochim. Biophys. Acta. 1787 (2009) 1324–1333. doi:10.1016/j.bbabio.2009.01.019.
[34] R.M. Denton, Regulation of mitochondrial dehydrogenases by calcium ions, Biochim. Biophys. Acta. 1787 (2009) 1309–1316. doi:10.1016/j.bbabio.2009.01.005.
[35] L.S. Jouaville, P. Pinton, C. Bastianutto, G.A. Rutter, R. Rizzuto, Regulation of mitochondrial ATP synthesis by calcium: evidence for a long-term metabolic priming, Proc. Natl. Acad. Sci. U. S. A. 96 (1999) 13807–13812.
[36] C. Calcabrini, U. Mancini, R. De Bellis, A.R. Diaz, M. Martinelli, L. Cucchiarini, P. Sestili, V. Stocchi, L. Potenza, Effect of extremely low-frequency electromagnetic fields on antioxidant activity in the human keratinocyte cell line NCTC 2544, Biotechnol. Appl. Biochem. 64 (2017) 415–422. doi:10.1002/bab.1495.
[37] R. Sadeghipour, S. Ahmadian, B. Bolouri, Y. Pazhang, M. Shafiezadeh, Effects of extremely low-frequency pulsed electromagnetic fields on morphological and biochemical properties of human breast carcinoma cells (T47D), Electromagn. Biol. Med. 31 (2012) 425–435. doi:10.3109/15368378.2012.683844.
[38] A.F. Santidrian, A. Matsuno-Yagi, M. Ritland, B.B. Seo, S.E. LeBoeuf, L.J. Gay, T. Yagi, B. Felding-Habermann, Mitochondrial complex I activity and NAD+/NADH balance regulate breast cancer progression, J. Clin. Invest. 123 (2013) 1068–1081. doi:10.1172/JCI64264.
[39] J. Park, C.M. Kusminski, S.C. Chua, P.E. Scherer, Leptin receptor signaling supports cancer cell metabolism through suppression of mitochondrial respiration in vivo, Am. J. Pathol. 177 (2010) 3133–3144. doi:10.2353/ajpath.2010.100595.

Figure legends

Fig. 1. The exposure to the specific electromagnetic wave inhibits the proliferation of human cancer and healthy cells. After four days of growth in standard condition (ctrl) or in presence of ELF-EMF at the indicated frequencies (ELF), MDA-MB-231 and MSTO-211H cancer cells and their non malignant counterpart MCF-10A and Beas-2B cells were subjected to crystal violet assay; HUVEC cells were analysed by BrdU incorporation. The values of the treated cells are expressed as the percentage of their respective controls (ctrl). The data represent the means ± SEM of three independent experiments. *$p < 0.05$ compared to the control.

Fig. 2. The ELF-EMF affects the proliferation rate and the cell cycle of the human cancer cell lines. After incubation in presence or absence of the specific irradiation (6 Hz for MDA-MB-231 and 16 Hz for MSTO-211H) for the indicated time,the cells were subjected to BrdU assay (A) or crystal violet staining (B, C).The analysis of cell cycle (D, E) was carried out after two days of exposure; representative histograms are shown in (D) and the mean of three experiments is plotted in (E). The values of the treated cells (ELF) are expressed as the percentage of their respective controls (ctrl). The data represent the means ± SEM of three independent experiments. *$p < 0.05$ compared to the control.

Fig. 3. The ELF-EMFaffects calcium fluxes. The cells were subjected to BrdU assay after two days of incubation in standard growth medium with calcium (GM), in medium without calcium (W/O CA), or in GM with the addition of 10 µM nifedipine (NIF), 10 µM verapamil (VER), 10 µM BAPTA-AM. The treatments were carried out in presence (ELF) or absence (ctrl) of ELF-EMF at the specific frequencies. The data are expressed as the means ± SEM of three independent experiments. *$p < 0.05$ compared to GM ctrl; ns: not significant.

Fig. 4. ELF-EMF enhances the expression of the respiratory chain and ATP synthase. (A) Real time analysis of COX2, COX4, MT-ATP6 and ATP5B subunits transcript expression in control and cells treated at the specific frequencies. Fold changes versus control are plotted on the

graphs. (B) Protein analysis of complex I, II, III, IV and ATP synthase (AS) in control and treated cells. Bands were quantified, normalized for loading control and data plotted on graph as values relative to control. All data represent the mean ± SEM of three independent experiments. *$p < 0.05$ compared to control.

Fig. 5. ELF-EMF induces the mitochondrial respiration and the production of ROS. After two days of exposure to specific frequencies of ELF-EMF (ELF) the mitochondrial membrane potential was assessed by JC-1 cytofluorimetric evaluation (A). Representative images from the cytofluorimetric analysis are shown in the left panel and the results from three separate experiments are plotted in the right panel, the FL2/FL1 ratio was calculated and the values were expressed as a percentage of the control (ctrl). (B) Mitochondrial ATP levels were measured by a chemiluminescence-based assay. (C) Intracellular LDH activity was measured spectrophotometrically and expressed as µmol NADH/min/mg prot. (D) The intracellular levels of ROS were measured by fluorimetric evaluation of the DCFDA-AM probe. Cells were treated with 100 µM menadione, which is a known generator of ROS, as positive control of the assay The results from three separate experiments are plotted on graph, where the data are expressed as the means ± SEM. *$p < 0.05$ compared to the control.

Fig. 6. The exposure to specific frequencies of ELF-EMF changes the conversion of energy of the target cells. A working model of the molecular mechanisms underlying the effects of the electromagnetic radiation on metabolism and growth of cancer cells. (A) The different transformation of energy (E) from nutrients into work (W) keeps the cells in equilibrium between the quiescent and the proliferating status. (B) ELF-EMF changes the conversion of energy, because when the cells are exposed to their resonant frequency, the increased demand for ATP necessary to balance the increased ion fluxes shifts the equilibrium at the expenses of duplication.

Supporting Information

Additional methods may be found in the supplementary information of this article.

Legend for supplemental illustration

Figure S1. The experimental setup

Figure S2. Representative western blots. Proteins from mitochondrial extracts were probed with the OXPHOS Human WB Antibody Cocktail against Complex I (C I), Complex II (C II), Complex III (C III), Complex IV (C IV), and ATP synthase subunit alpha (AS). The same membranes were also probed with an antibody against VDAC for loading control and the quality of mitochondrial purification was checked with an antibody against actin, which did not detect this cytosolic protein. Molecular weights are shown on the left.

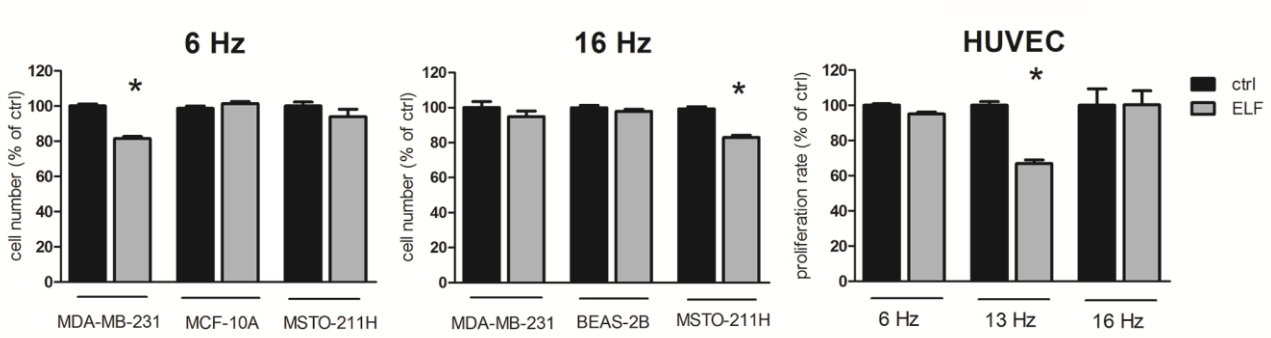

Figure 1

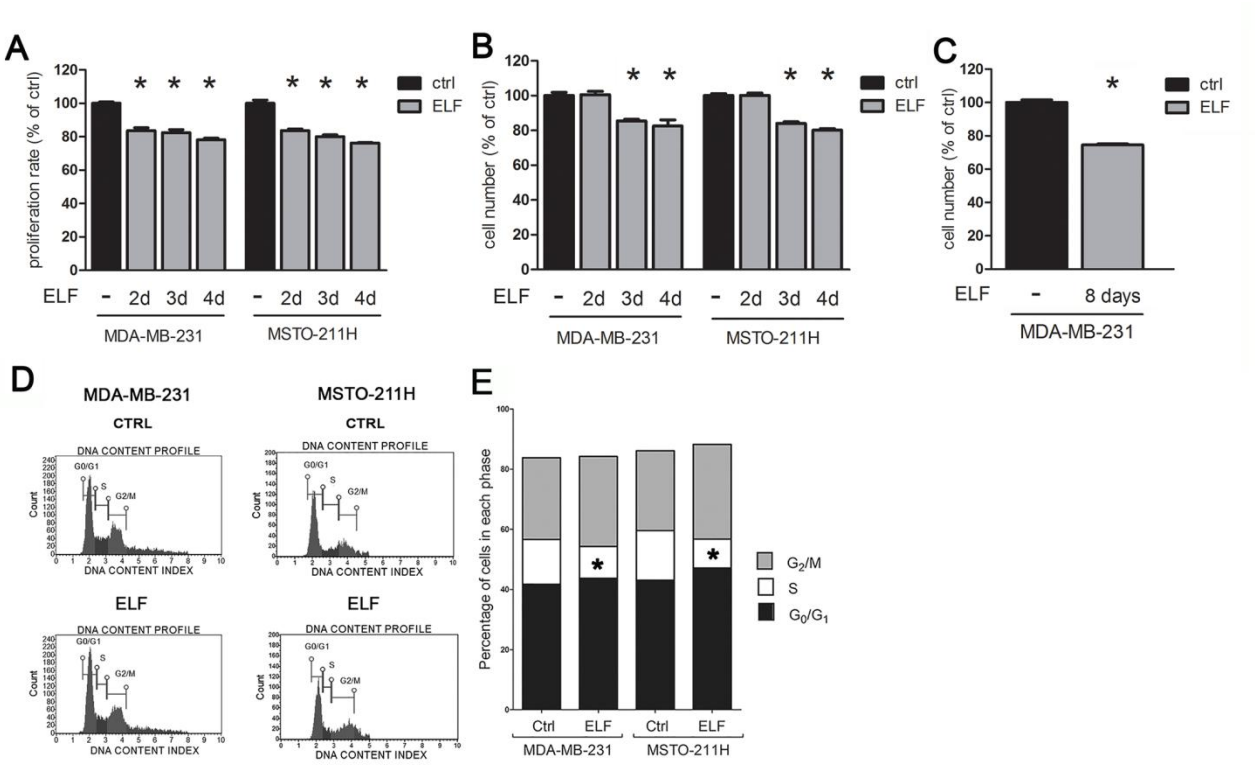

Figure 2

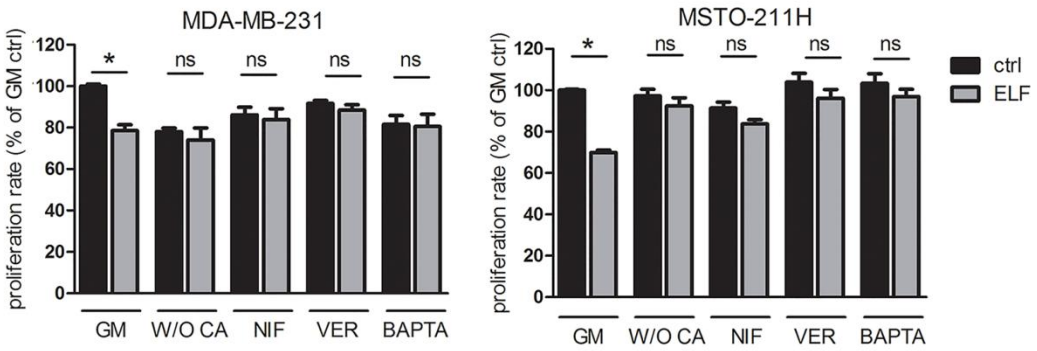

Figure 3

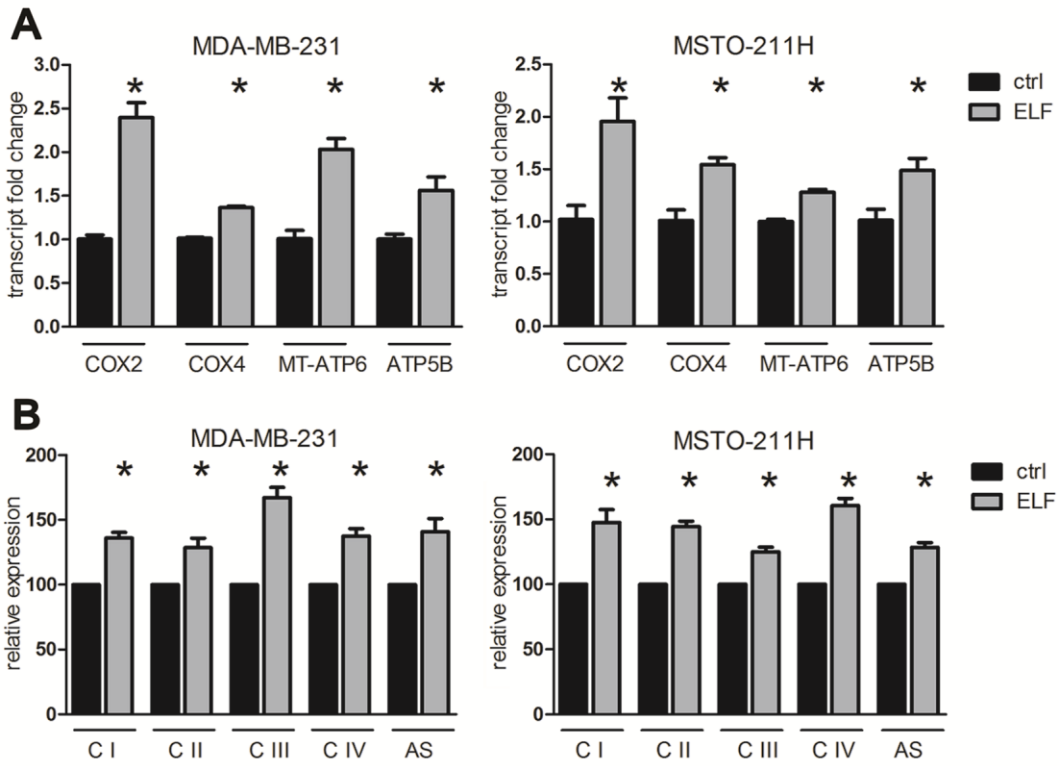
A
MDA-MB-231
MSTO-211H
transcript fold change
3.0
2.5
2.0
1.5
1.0
0.5
0.0
COX2
COX4
MT-ATP6
ATP5B
ctrl
ELF
B
relative expression
200
150
100
50
0
C I
C II
C III
C IV
AS

Figure 4

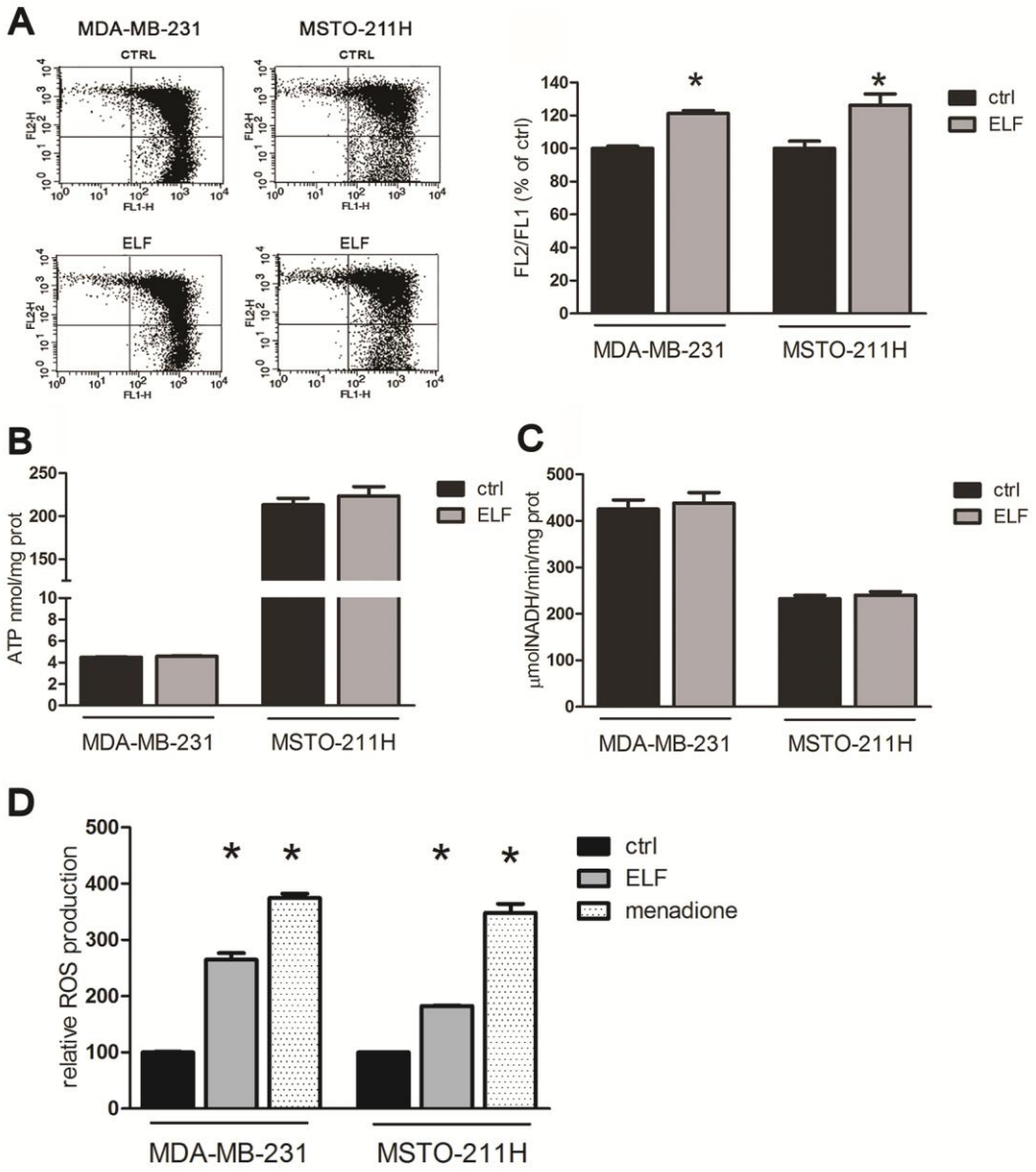
A
MDA-MB-231
MSTO-211H
CTRL
CTRL
ELF
ELF
FL2-H
FL1-H
FL2/FL1 (% of ctrl)
ctrl
ELF
MDA-MB-231
MSTO-211H
B
ATP nmol/mg prot
ctrl
ELF
MDA-MB-231
MSTO-211H
C
µmolNADH/min/mg prot
ctrl
ELF
MDA-MB-231
MSTO-211H
D
relative ROS production
ctrl
ELF
menadione
MDA-MB-231
MSTO-211H

Figure 5

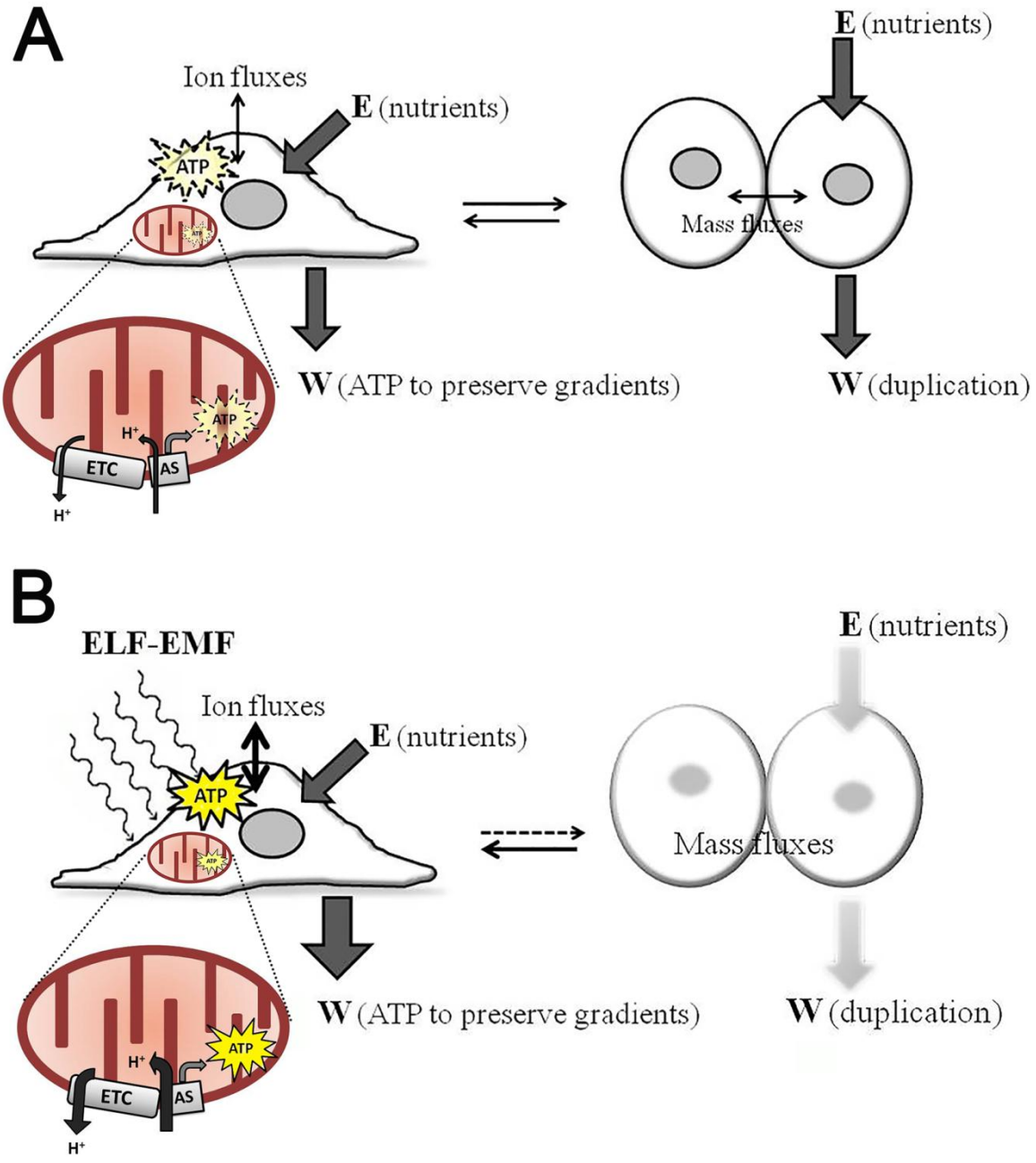
A
Ion fluxes
E (nutrients)
ATP
E (nutrients)
Mass fluxes
W (ATP to preserve gradients)
W (duplication)
H+
ATP
ETC
AS
H+
B
ELF-EMF
Ion fluxes
E (nutrients)
ATP
E (nutrients)
Mass fluxes
W (ATP to preserve gradients)
W (duplication)
H+
ATP
ETC
AS
H+

Figure 6

Figure S1

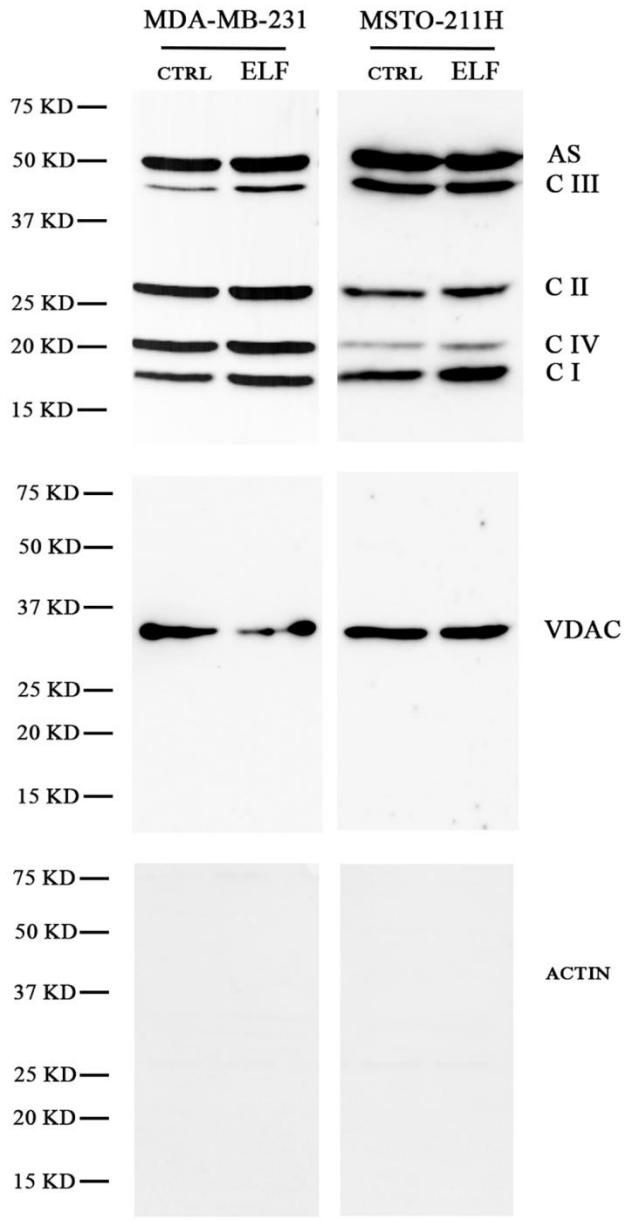
MDA-MB-231
MSTO-211H
CTRL
ELF
CTRL
ELF
75 KD
50 KD
37 KD
25 KD
20 KD
15 KD
AS
C III
C II
C IV
C I
VDAC
ACTIN

Figure S2